Issue 62

GAṆANAM (गणनम्)

JANUARY 2026

HIGH PERFORMANCE COMPUTING NEWSLETTER
INSTITUTE FOR PLASMA RESEARCH, GANDHINAGAR

Inside this issue:
(3 pages)

Effects of Localization on Pinned Solitons in Yukawa Fluids	1
ANTYA High Performance Computing Documentation Portal	2
ANTYA Usage Statistics and Observed workloads - Dec 2025	3

Effects of Localization on Pinned Solitons in Yukawa Fluids

Debkumar Chakraborty (PDF, Basic Theory and Simulation Division, IPR)
Email: deb.chakraborty@ipr.res.in

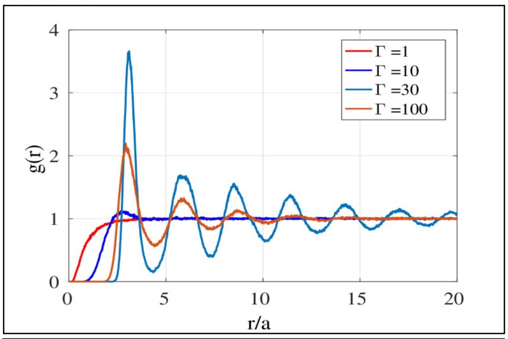

FIGURE 1: The plot of the radial function ***g(r)*** for different values of the parameter Γ for *κ* =1.0.

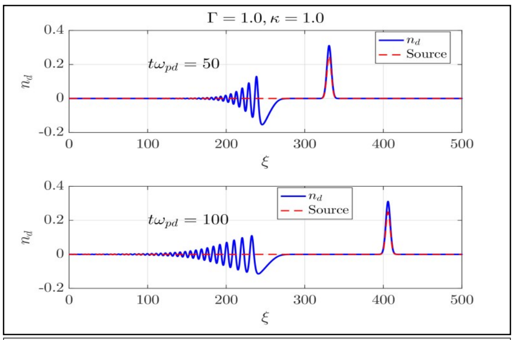

FIGURE 2: The snapshots of pinned solitons evolution at different time for Γ = 1, κ = 1 and the other parameters are f_0 = 0.1, v_d = 2.5 , and δ = 4.

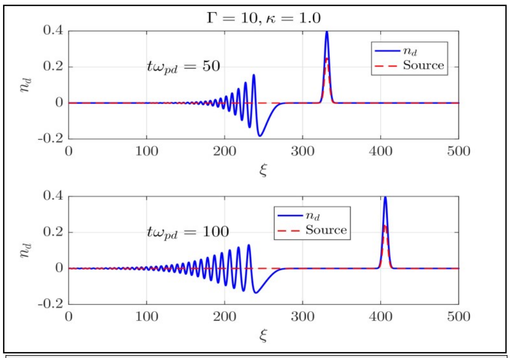

FIGURE 3: The snapshots of pinned solitons evolution at different time for Γ = 10, κ = 1 and the other parameters are f_0 = 0.1, v_d = 2.5 , and δ = 4.

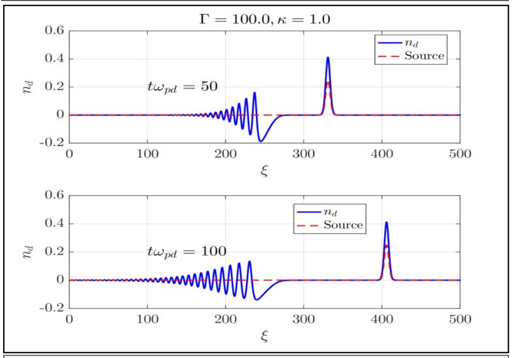

FIGURE 4: The snapshots of pinned solitons evolution at different time for Γ = 100, κ = 1 and the other parameters are f_0 = 0.1, v_d = 2.5 , and δ = 4.

Pinned solitons are stationary nonlinear wave structures that arise when a localized external source continuously excites a dispersive medium [1]. Unlike freely propagating solitons [2-5], which travel without changing shape, pinned solitons remain spatially confined near the forcing region while maintaining a localized waveform [6]. Such structures are particularly relevant in Yukawa and dusty plasma systems, where screening and strong inter-particle coupling significantly modify the balance between nonlinearity and dispersion. A convenient theoretical framework for describing these waves is provided by the Forced Korteweg–de Vries (fKdV) equation, in which nonlinear steepening, dispersion, and external forcing are incorporated through coefficients that depend explicitly on the thermodynamic properties of the medium [1]. Consequently, the amplitude and width of pinned solitons are strongly influenced by the microscopic state of the system.

In strongly coupled Yukawa fluids, the microstructural organization of particles plays a central role in determining macroscopic wave behaviour. This structure is quantified through the pair correlation function *g(r)* which measures how the presence of one particle affects the probability of finding another at a distance *r* . Deviations of *g(r)* from unity indicate strong correlations and the emergence of spatial ordering. As the coupling strength increases, the system undergoes a transition from a weakly coupled, fluid-like state [7] to a localized or quasi-solid phase. This transition is closely linked to the thermodynamic compressibility parameter α, which characterizes the response of the medium to compression. Changes in the magnitude or sign of α reflect reduced compressibility and enhanced rigidity, both of which have important consequences for nonlinear wave dynamics.

To identify the onset of localization, molecular dynamics simulations are carried out using the LAMMPS package on the HPC–ANTYA cluster at the Institute for Plasma Research (IPR). A two-dimensional Yukawa system consisting of 10,000 particles with periodic boundary conditions is evolved until thermal equilibrium is achieved for prescribed values of the coupling strength Γ and screening parameter κ [8]. Particle configurations sampled over many time frames are then used to compute the pair correlation function *g(r)* Figure-1 presents *g(r)* for different coupling strengths, Γ=*1,10,30,and 100*. For weak coupling (Γ=*1*), *g(r)* remains nearly flat, indicating the absence of short-range order characteristic of a weakly coupled regime. As the coupling strength increases, a pronounced peak emerges around Γ ≈ 10, signaling the onset of strong correlations and particle localization. For higher coupling strengths (Γ = *30 and 100*), the peak becomes increasingly prominent, reflecting the development of well-defined local structure. These results clearly demonstrate a transition from a weakly coupled state to a localized, strongly coupled phase occurring near Γ~10. The influence of this localization transition is incorporated into the nonlinear wave description through the fKdV equation [1],

$$\phi_\tau + A\phi\phi_\xi + B\phi_{\xi\xi\xi} = CS_\xi \quad \text{———(1)}$$

where $S(\xi,\tau) \equiv S(\xi + M\tau)$ represents the external source with $M = V - v_d$ and v_d is the normalized source velocity. Moreover, A, B and C represent the coefficients of nonlinear steepening, dispersion, and external forcing, respectively given by [1].

$$A = \left[\alpha\mu/\left(2V(V^2-\alpha)\right) - 3\mu V^2/(V^2-\alpha) + (V^2-\alpha)h_2/(2Vh_1)\right],\ B = [(V^2-\alpha)\mu/(2V h_1)],\ C = B/\mu. \quad \text{——(2)}$$

These coefficients depend explicitly on the compressibility parameter α, which is defined as $\alpha = \frac{\gamma\,\tilde{\alpha}}{3\Gamma}$, and the adiabatic compressibility modulus is [3,4]

$$\gamma\,\tilde{\alpha} = \tilde{\alpha} + \frac{\left(p - \Gamma\frac{\partial p}{\partial \Gamma}\right)^2}{\left(u - \Gamma\frac{\partial u}{\partial \Gamma}\right)}. \quad \text{———(3)}$$

As localization strengthens, α departs from its weak-coupling behaviour, reflecting reduced compressibility and increased stiffness of the medium. In this way, the microscopic structural information encoded in g(r) is consistently linked to the macroscopic nonlinear response governing pinned soliton dynamics.

The fKdV equation is solved numerically using a pseudospectral method, in which spatial derivatives are evaluated in Fourier space, nonlinear terms are computed in real space with appropriate dealiasing, and time integration is performed using an explicit scheme. This approach enables accurate resolution of nonlinear wave evolution with high spectral accuracy [5]. The simulations reveal the formation of stationary pinned solitons through a balance of forcing, nonlinearity, and dispersion. In the weakly coupled regime, both the soliton amplitude and width vary significantly with the coupling strength Γ. However, as the system approaches the localized regime—identified independently by the emergence of pronounced peaks in g(r) (Figure 1) and by changes in the compressibility parameter—the soliton properties begin to saturate [1,8].

To further elucidate this behaviour, pinned solitons are excited dynamically from rest using an arbitrary moving Gaussian source [1,9]

$$S(\xi,\tau) = f_0 \exp\left[-\frac{(\xi - 256 + M\tau)^2}{\delta^2}\right]. \quad \text{———(4)}$$

Where, f_0, δ are respectively the amplitude and width of the source. No initial perturbation is imposed; instead, the wave structure develops solely due to the action of the moving source. The resulting pinned solitons generated at Γ=*1,10 and 100* shown in Figures 2–4, exhibit nearly identical spatial profiles after Γ~10. This demonstrates that beyond the localization threshold, further increases in coupling strength do not significantly modify the soliton amplitude or width. The saturation of soliton properties therefore coincides with the onset of particle localization, as independently indicated by both the behaviour of the pair correlation function and the thermodynamic compressibility [1].

Although wake structures are observed behind the moving source in Figures 2–4, the primary focus of the present study is on pinned solitons. A detailed investigation of wake dynamics in the strongly coupled regime is therefore left for future work. Overall, these results establish a direct and physically transparent connection between particle-scale localization and the macroscopic stability of pinned solitons in strongly coupled Yukawa fluids.

References:

1) P. Kumar, D. Chakraborty and D. Sharma, *Contributions to Plasma Physics*, e70066, (2025), https://doi.org/10.1002/ctpp.70066.
2) P. Kumar and D. Sharma, *Physics of Plasmas* 28, 083704 (2021).
3) S. Dalui, P. Kumar, P. Jana, and D. Sharma, *Physics of Plasmas* 32, 083701 (2025).
4) P. Kumar and D. Sharma, *Journal of Plasma Physics* 91, E61 (2025).
5) P. Kumar and D. Sharma, *Physics of Plasmas* 30, 033702 (2023).
6) A. Mistri, D. Chakraborty, and S. Ghosh, *Physics of Fluids* 35, 076103 (2023).
7) P. Kumar and D. Sharma, *Physics of Plasmas* 27, 063703 (2019).
8) P. Kumar and D. Sharma, *Contributions to Plasma Physics* 64, e202400026 (2024).
9) D. Chakraborty, A. Biswas, and S. Ghosh, *Physics of Plasmas* 29, 122304 (2022).

ANTYA High Performance Computing Documentation Portal

ANTYA High Performance Computing (HPC) cluster at the Institute for Plasma Research (IPR), established to meet the growing computational demands of scientific and technical research. To ensure effective and efficient utilization of this facility, an in-house documentation website has been developed. This article provides a concise overview of that documentation portal, its structure, and its purpose. The ANTYA documentation website is organized around a clear, user-centric navigation structure. Each section corresponds to a typical stage in an HPC user's workflow, from initial access to job execution. The portal serves as the primary reference for users, reducing dependency on direct support and promoting self-sufficiency.

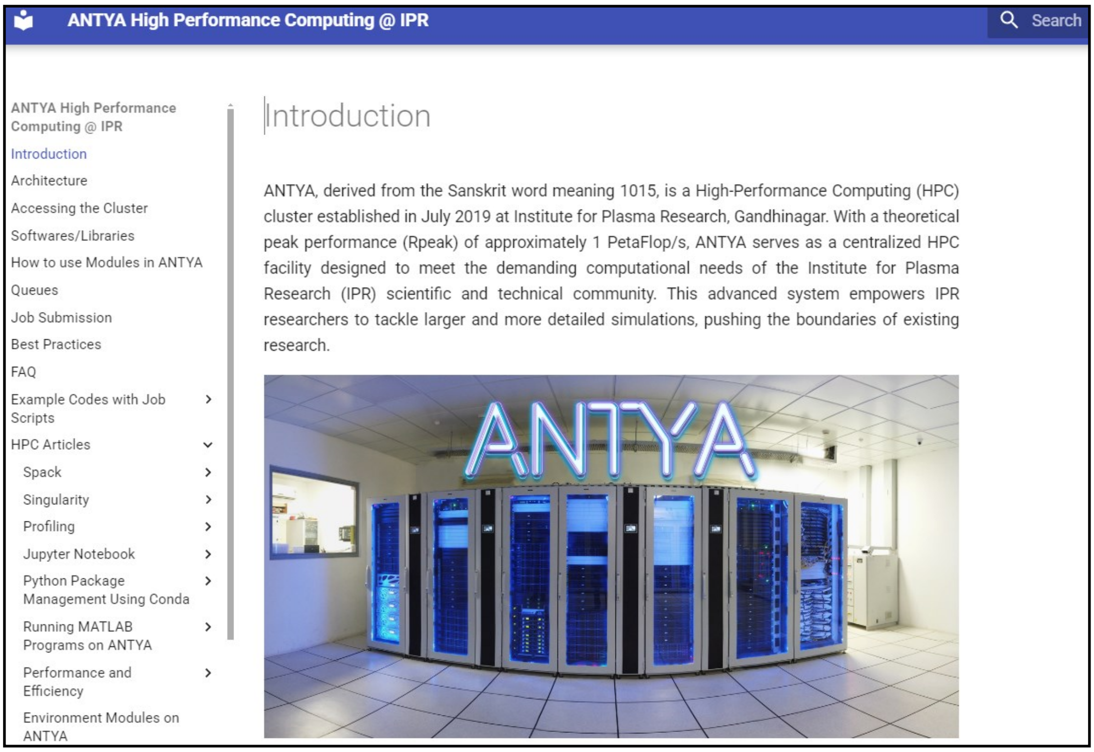

Source: https://hpctutorial.ipr.res.in/ANTYA/

1) Introduction Section
This section introduces ANTYA, its background, capabilities, and role within IPR. It provides new users with essential context about the system, its scale, and intended usage.

2) Architecture
The Architecture section describes the hardware and system design of the cluster, including compute nodes, memory, interconnects, and storage.

3) Accessing the Cluster
The ANTYA cluster consists of Linux-based machines. User access to the cluster is provided through a small number of designated login nodes, which serve as the entry point to the system. Users can log in to these nodes to prepare, submit, and monitor their computational jobs. The cluster can be accessed from any computer connected to the IPR internal network, ensuring convenient and secure availability for authorized users

4) Softwares and Libraries
The Softwares/Libraries section lists the compilers, numerical libraries, MPI implementations, and scientific and commercial applications available on the cluster.

5) Using Modules in ANTYA
This section introduces the environment module system used to manage software on ANTYA. It explains how users can load, unload, and switch between software environments, which is essential for compiling and running applications correctly.

6) Queues
The Queues section describes the job scheduling system and available queues, along with their resource limits and intended use cases. This helps users select appropriate queues and optimize job turnaround time.

7) Job Submission
The Job Submission section provides guidance on writing and submitting job scripts, requesting resources, and monitoring jobs. Practical examples help users understand both serial and parallel job execution workflows.

8) FAQ
The FAQ section addresses common user questions related to access, job failures, and software usage, enabling quick resolution of routine issues.

9) Example Codes with Job Scripts
This section provides sample programs along with corresponding job scripts, serving as templates that users can adapt for their own applications.

10) HPC Articles
The HPC Articles section hosts technical articles, case studies, and best-practice notes related to HPC usage at IPR. It also maintains a list of articles published to date, serving as a growing knowledge repository for the user community.

For detailed, continuously updated information, users are encouraged to refer to the ANTYA documentation portal: https://hpctutorial.ipr.res.in/ANTYA/

ANTYA Utilization: DECEMBER 2025

ANTYA DAILY OBSERVED WORKLOAD

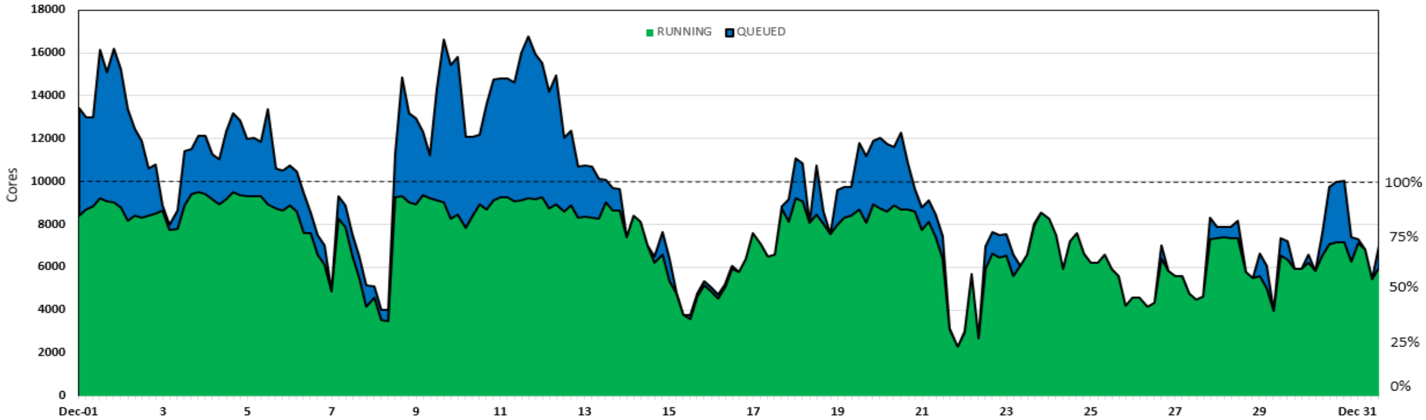

ANTYA HPC Users' Statistics

December 2025

Total Successful Jobs~ 970

> Top Users (Cumulative Resources)

- **CPU Cores** Gopal Mailapalli
- **Walltime** Kaushal Parikh
- **Jobs** Jugal Chowdhury

ANTYA Usage, Updates and News

- **Scheduled Downtime**: There was no downtime of ANTYA for December 2025.
- **Job Submissions**: The highest job loads were observed in the *serialq*, *regularq*, *mediumq*, *longq and ansysq* queues, reflecting sustained user activity across multiple workloads in various queues.
- **Cluster Utilization**: The system maintained an average utilization of ~72.68% and peak utilisation of ~95.09%.

Packages/Applications Installed: No new modules have been installed this month. To view list of available modules.
> module avail

Other Recent Work on HPC

Design of a Plasma-Based Yagi–Uda Antenna Array for Beam Steering Applications	Manisha Jha
Shear Induced Suppression of Electromagnetic Blob Merging: A Nonlinear Threshold Framework	Souvik Mondal
Numerical Investigation of Electromagnetic Wave Mode Destabilization by Non-thermal Beam-Plasma Electron distributions	Pooja
A Global Gyrokinetic Study of Short Wavelength Ion Temperature Gradient Modes in the Presence of Reversed Magnetic Shear in ADITYA-U Tokamak	Gopal Krishna M
DEGAS-2 Based Parametric Modeling of Gas Puff Imaging on the ADITYA-U Tokamak	Ruchi Varshney
A numerical study of MHD drift-tearing mode for Aditya-U tokamak	Vinod Saini
Simulation of Resonance Flux and Neo-Toroidal Viscosity Torque in Aditya-U under External Magnetic Perturbation	Ananya Kundu
Study of intrinsic toroidal rotation in the Scrape-Off Layer of inboard-limited Aditya-U plasmas	Arzoo Malwal
Fluid Modeling and Simulations of Plasma Flows in the Scrape-off Layer of Magnetic Confinement Fusion Experiments	Devendra Sharma

Acknowledgement

Join the HPC Users Community

hpcusers@ipr.res.in

If you wish to contribute an article in GAṆANAM, please write to us.

GAṆANAM (गणनम्)

Contact us

HPC Team (*hpcteam@ipr.res.in*)
Computer Division, IPR